Three-Dimensional Modeling and Analysis of a Human Ankle Joint

Muhammad Hanif Ramlee, Mohammed Rafiq Abdul Kadir
Medical Devices and Technology Group
Faculty of Biosciences and Medical Engineering
Universiti Teknologi Malaysia
81310 Johor Bahru, Johor, Malaysia
mhanif008@gmail.com, rafiq@biomedical.utm.my

Habibollah Harun
Faculty of Computing
Universiti Teknologi Malaysia
81310 Johor Bahru, Johor, Malaysia
habib@utm.my

Abstract— **Developing an accurate finite element model of an ankle joint is a challenging task and time consuming. Several steps were utilized to minimize over-simplification of the model as can be found in literature. The objective of this study is to biomechanically analyzed, via the finite element method, a more precise model of a human ankle joint. Computed Tomography dataset of a healthy male volunteer was used to reconstruct a detailed three-dimensional model of an ankle joint. The bone models were segmented into two types of bones - cortical and cancellous according to the Hounsfield unit. The ankle model consists of tibia, fibula, talus, calcaneus, cuboid, navicular, three cuneiforms and five metatarsals bones. The cartilages were constructed by offsetting bone layer and were assigned with the Mooney-Rivlin mechanical behavior. To complete the joint, thirty-seven ligaments were modeled using linear spring elements. Finite element method was used to analyze the effect of seven different forces applied on the tibia. Displacements of the model were compared with previous experimental work. The results showed that the predicted displacement of the medial cuneiform bone was similar to those experimental work reported by others.**

Keywords—finite element, biomechanics, ankle, CT scanning

I. INTRODUCTION

Ankle joint is a musculoskeletal joint between the distal tibia, distal fibula and talus bones. The force acted on this joint is very complex. During the swing phase of a gait cycle, the force is equal to 10% of the body weight and about 50% during the stance phase [1-2]. There are four types of motion associated with the ankle joint – plantar flexion, dorsi flexion, inversion and eversion. The joint is susceptible to fracture under extreme load and can dislocate due to overstrain.

The use of finite element model for analysis of human joints have received significant attention as it can provide insight into the behavior of the joint under various loading configurations. Parameters such as internal stresses and displacements that would otherwise be impossible to measure in-vivo, could be predicted via this technique [3-6]. It is highly efficient in terms of cost and time, and has been proven to produce reliable predictions.

From our extensive search of the literature, there were nine reports analyzing the ankle joint via finite element method [3, 6-13]. Some of these reports simplified the material properties of bone by assigning a single value for both cortical and cancellous bones [3, 9-10, 12]. Others assigned a single value for all 37 ligaments associated with the ankle joint [10, 12-13], or did not model the cartilages [7-8]. Those who model the cartilages assigned an isotropic behavior which is an over simplification of the soft tissue [10, 12]. Thus, a new method was developed to create a more accurate representation of the ankle joint.

Due to the complexity of the ankle anatomy, developing a good finite element model of an ankle joint is both challenging and time consuming. The technique consisted of several steps including the realization of soft tissues namely the cartilages and ligaments as well as segmentation of cortical and cancellous bones. The detailed model was then tested under axial loading where the results obtained were compared with other experimental work from literature.

II. MATERIALS AND METHODS

A. Modeling of Bones

Computed Tomography (CT) image dataset of a healthy 21 year old male volunteer with a height of 173 cm and weight 70kg was obtained from Hospital Tengku Ampuan Afzan, Kuantan, Pahang, Malaysia. The CT dataset consisted of 225 slices of the lower limb including the knee and the foot, with a slice thickness of 1.5mm. The dataset was loaded into an image processing software Mimics (Materialise, Leuven, Belgium), followed by a segmentation procedure. A Hounsfield unit of 700 [14] was set to distinguish between cortical and cancellous bones (Fig. 1). The semi automatic procedure was done twice to select cortical (Hu > 700) and then the cancellous (Hu < 700). Three dimensional model will be automatically developed representing the cortical and the cancellous bone. A Boolean operation was used to remove overlapping of the models and to ensure smooth transition from cortical to cancellous.

This research is supported by the Ministry of Higher Education Malaysia (MOHE) and was conducted in collaboration with the Research Management Centre (RMC), Universiti Teknologi Malaysia (UTM).

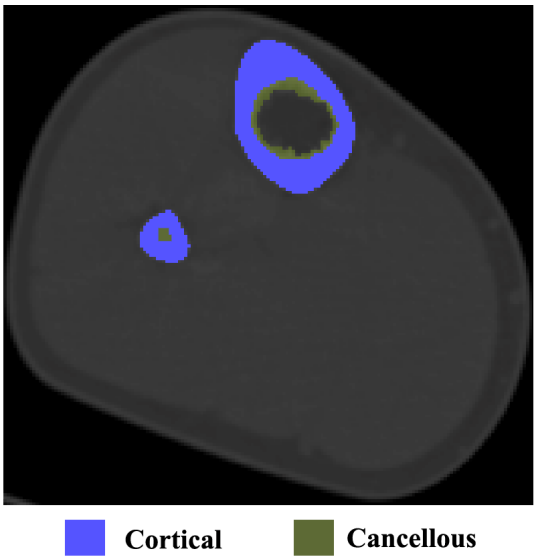

Fig. 1 Cortical and cancellous regions for the tibia and fibula bone

By now, the developed 3D model covers both the knee and ankle joint. Since the analysis will concentrate on the ankle joint, a specific region of interest was set where the tibia bone was cut approximately 20 cm above the medial tibia malleolus. The completed ankle model consists of tibia, fibula, talus, calcaneus, cuboid, navicular, three cuneiforms, and five metatarsals bones. All the bone were converted into surface triangular mesh and saved in stereolithographic (STL) format.

B. *Modeling of the Cartilages*

Articular cartilage is a specialized soft tissue with smooth surface to minimize friction between contacting bones. A uniform cartilage thickness size of 1 mm was set by extruding the surface of the tibia, fibula, calcaneus and talus bones (Fig. 2) [15-16]. This offsetting process was performed manually in Mimics. All intersections between cartilages and bones were removed through boolean operations. A hyper-elastic Mooney-Rivlin properties were assigned to the cartilage with the coefficients of C_{01}=0.41 MPa and C_{10}=4.1 MPa [17]. The Mooney-Rivlin properties has been reported to better represent the properties of the cartilage [18].

C. *Modeling of the Ligaments*

Ligament is a fibrous tissue that connects two bones across a joint which functions as a guide to joint movement and maintain joint congruency. In the model, a total of 37 ligaments were modelled using linear spring elements [18-19]. The insertion point of each ligament was estimated based on a reference anatomy book [20]. For the mechanical behavior of the respective ligaments, stiffness parameter ranging from 40 to 400 N/mm was assigned as shown in Table I [7, 21-24].

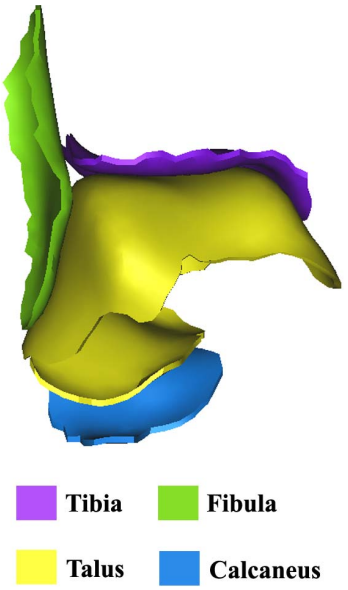

Fig.2 Three-dimensional stucture of the cartilages

In cases where ligamental properties could not be obtained from literature, the value was assumed to be similar to the closest known ligament properties. In order to properly distribute the load transfer of the ligament to the bone, each ligament was represented with four parallel linear springs [18, 25].

D. *Finite Element Modeling*

The STL files of the bones and cartilages were imported into 3-Matic software (Materialise, Leuven, Belgium). In this process, triangular patches were changed after automatic optimization. Next, a finite element software, Marc.Mentat (MSC.Software, Santa Ana, CA) software was used to convert the triangular surface mesh into linear first order tetrahedral elements. The elastic modulus value and Poisson's ratio for the cortical bone was set to 7300 MPa and 0.3 [8, 26], whilst the cancellous bone was set to 1100 MPa and 0.3 respectively [27].

E. *Finite Element Analysis*

The finite element method was used to biomechanically analyze the effect of seven different forces on the ankle joint. The model was compressed at the tibia with vertical forces ranging from 100 to 700 N (Fig. 3). These forces were simulated as these have been used in previous reported experiment [6]. To prevent rigid body motions, the metatarsals and calcaneus bones were fixed in all degrees of freedom as shown in Fig. 3.

Vertical deformation of the model from the finite element analysis were compared to the results from a cadaver study from previous literature [6]. Since the transducer was placed near the medial cuneiform, the comparison was made based on the displacement at that particular bone.

TABLE I. STIFFNESS OF LIGAMENTS

Ligaments represented in the models	**Stiffness (N/mm)**
Interosseous membrane (4 ligaments)	400 [21]
Anterior tibiofibular (distal)	78 [22]
Posterior tibiofibular (distal)	101 [23]
Anterior talofibular	90 [22]
Posterior talofibular	70 [24]
Calcaneofibular	70 [24]
Anterior tibiotalar	70 [22]
Posterior tibiotalar	80 [22]
Tibiocalcaneal	122 [22]
Tibionavicular	40 [22]
Interosseous talocalcaneal	70 [21]
Lateral talocalcaneal	70 [24]
Medial talocalcaneal	70 [24]
Posterior talocalcaneal	70 [24]
Dorsal talonavicular (2 ligaments)	70 [22]
Calcaneonavicular (dorsal & plantar)	70 [24]
Calcaeocuboid (dorsal & short plantar)	70 [24]
Cuboideonavicular (dorsal & plantar)	70 [22]
Cuneonavicular (dorsal & plantar)	70[a]
Intercuneiform (dorsal & plantar)	70[a]
Tarsometatarsal (dorsal & plantar)	70[a]
Metatarsal (dorsal & plantar)	70[a]
Medial plantar fascia	200 [7]
Central plantar fascia	230 [7]
Lateral plantar fascia	180 [7]
Long plantar	70 [21]

[a]Assumed from neighbouring ligaments

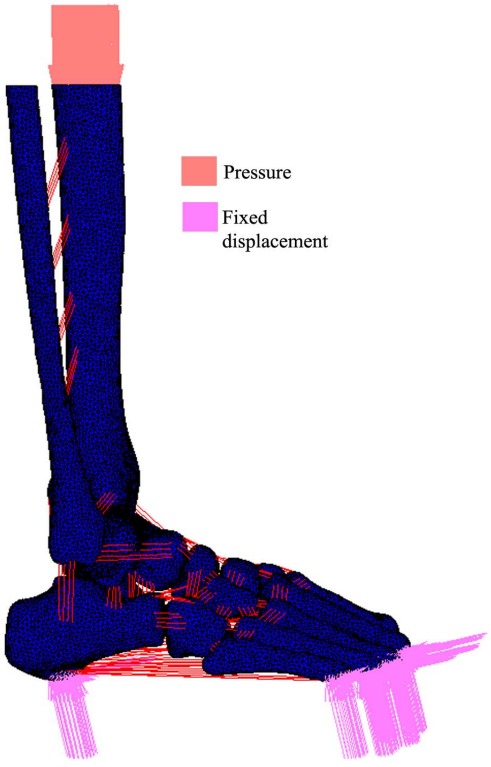

Fig. 3 Boundary conditions

III. RESULT AND DISCUSSION

A. Finite Element Model

The 3D finite element model of a human ankle joint is illustrated in Fig. 4. The model consists of 14 bones includes tibia, fibula, talus, calcaneus, navicular, cuboid, three cuneiforms, and five metatarsals. Other structures are five cartilages and 37 of the ligaments.

Due to lack of details and accurate data for the geometry of human body structure, several assumptions and simplifications were necessary. In our study, the mechanical properties of the cortical and cancellous bones were simplified as isotropic, homogenous and linear material properties. This simplification has been widely used in the previous reports [3-4, 6-10]. In addition, the insertion points of the ligaments were estimated from the literature and the simulated linear links is adequate to represent its function [18-19]. Another simplification used in this finite element model is the thickness of the cartilages was uniform in 1 mm. This process was taken due to the complexity of the soft tissue boundary and low resolution of CT images [15-16]. To construct structure of the soft tissue, the use of Magnetic Resonance Imaging (MRI) data is better than CT images.

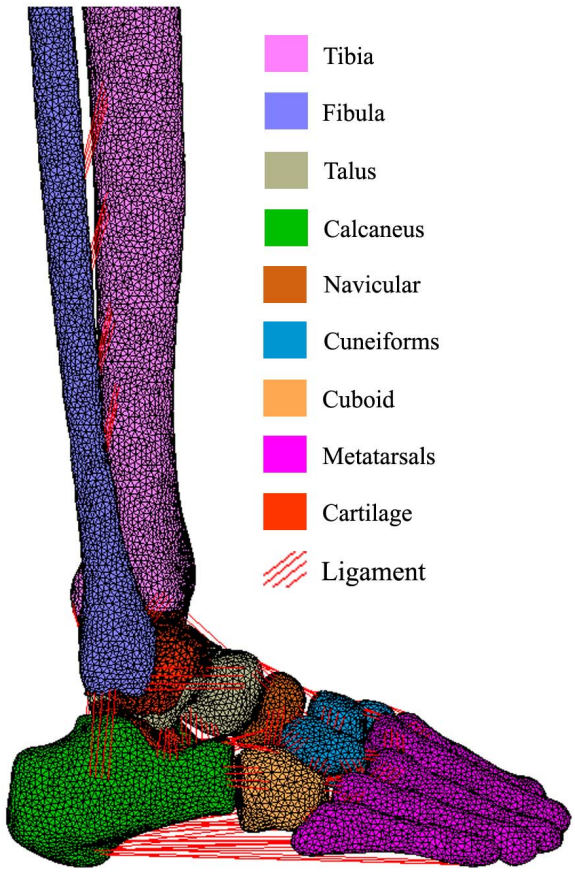

Fig. 4 Three-dimensional finite element model

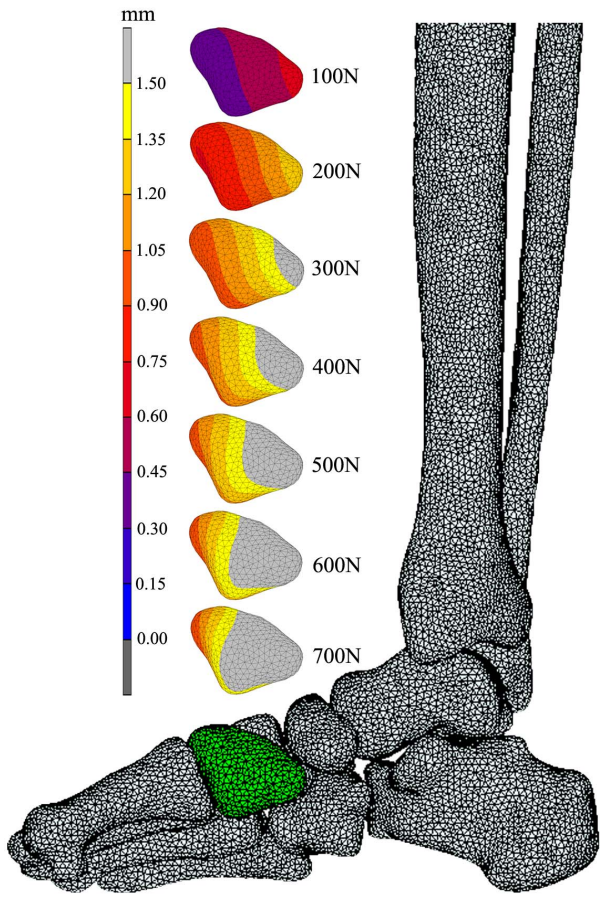

Fig. 5 Contour plot (vertical displacement) of medial cuneiform bone. Green colour indicates position of the bone in the finite element model.

B. *Finite Element Analysis*

Fig. 5 shows the contour plot (vertical displacement) of medial cuneiform bone and Fig. 6 is the graph explaining variations in the predicted displacement data using finite element analysis and experiment measurements. Generally, the vertical deformation were increased when increasing the vertical compression force. Maximum displacement for predicted and experimental were observed at 700 N of compression force applied, with value of 2.3 mm and 4.6 mm respectively [6]. From the Fig. 6, it could be seen the finite element results has lower magnitude than the experiment measurements.

The discrepancy of lower magnitude in the predicted data might be the simplification of linear spring element in the finite element model. The under-estimation of predicted model also causes by assumption of linear material properties of the cortical bone, cancellous bone, geometry of the cartilages and the absence of other soft tissue such as fat and skin. However, it should be noticed that the finite element model characteristics in term of the deformation of the medial cuneiform bone was similar to the experimental measurements.

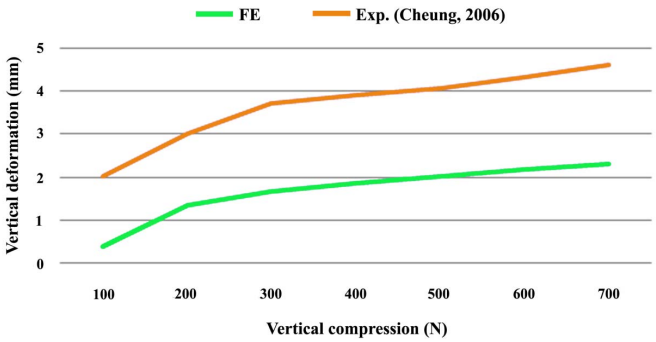

Fig. 6 The vertical deformation under compression loading obtained from previous experimental measurements and finite element predictions.

IV. CONCLUSION

The model of a human ankle finite element was successful reconstructed based on CT images data using Mimics, 3-matic and Marc.Mentat software. The model represents the cortical bone, the cancellous bone, the cartilages and the ligaments. Based on the results and presented discussions, it can be concluded that the finite element results were in coincident agreement with the experimental measurements in term of its vertical deformation at the medial cuneiform bone with maximum value of 2.3 mm and 4.6 mm respectively.

ACKNOWLEDGMENT

The authors would like thank to the Medical Devices and Technology Group, Faculty of Biosciences and Medical Engineering and Universiti Teknologi Malaysia for the valuable research facilities. This research is supported by the Ministry of Higher Education Malaysia (MOHE) and was conducted in collaboration with the Research Management Centre (RMC), Universiti Teknologi Malaysia (UTM).

REFERENCES

[1] F. C. Anderson and M. G. Pandy, "Static and dynamic optimization solutions for gait are practically equivalent," J. Biomec., vol. 34, pp. 153-161, 2001.

[2] A. Simkin, Structural analysis of the human foot in standing posture. Tel Aviv: Tel Aviv University, 1982.

[3] A. Gefen, "Simulations of foot stability during gait characteristic of ankle dorsiflexor weakness in the elderly," IEEE Transactions on Neural Systems and Rehabilitation Engineering, 2001.

[4] Z. Su, Z. Chen, Z. Wei, and Z. Xia, "Biomechanical analysis of large segmental bone repair with different fixation apparatuses," presented at the IEEE 3rd International Conference on Biomedical Engineering and Informatics (BMEI), 2010.

[5] A. Lesniewska, W. Choromanski, J. Deszcynski, and G. Dobrzynski, "Modeling and simulation of physical performance of a external unilateral mechatronic orthopaedic fixator-Bone system," Proceedings of the 28th IEEE EMBS Annual International Conference, pp. 1533-1536, 2006.

[6] J. T.-M. Cheung, M. Zhang, and K.N. An, "Effect of Achilles tendon loading on plantar fascia tension in the standing foot," Clinical Biomechanics, vol. 21, pp. 194-203, 2006.

[7] J. M. Iaquinto and J. S. Wayne, "Computational model of the lower leg and foot/ankle complex: application to arch stability," Journal of Biomechanical Engineering, vol. 132, 2010.
[8] T. X. Qiu, E.C. Teo, and W. Lei, "Finite element modeling of a 3D coupled foot-boot model," Medical Engineering & Physics, vol. 33, pp. 1228-1233, 2011.
[9] J. Yu, J.T. Cheung, Y. Fan, Y. Zhang, A.K. Leung, and M. Zhang, "Development of a finite element model of female foot for high-heeled shoe design," Clinical Biomechanics, vol. 23, pp. 31-38, 2007.
[10] K. Tao, D. Wang, C. Wang, X. Wang, A. Liu, C.J. Nester, and D. Howard, "An in vivo experimental validation of a computational model of human foot," Journal of Bionic Engineering, vol. 6, pp. 387-397, 2009.
[11] X. Liu and M. Zhang, "Redistribution of knee stress using laterally wedged insole intervention: Finite element analysis of knee-ankle-foot complex," Clinical Biomechanics, vol. 28, pp. 61-67, 2013.
[12] J. T.-M. Cheung, M. Zhang, A.K. Leung, and Y.B. Fan, "Three-dimensional finite element analysis of the foot during standing- a material sensitivity study," Journal of Biomechanics, vol. 38, pp. 1045-1054, 2005.
[13] X.-Q. Dai, Y. Li, M. Zhang, and J.T. Cheung, "Effect of sock on biomechanical responses of foot during walking," Clinical Biomechanics, vol. 21, pp. 314-321, 2006.
[14] Z. Yosibash, N. Trabelsi, and C. Milgrom, "Realiable simulations of the human proximal femur by high-order finite element analysis validated by the experimental observations," Journal of Biomechanics, vol. 40, pp. 3688-3699, 2007.
[15] S. A. Millington, M. Grabner, R. Wozelka, D.D. Anderson, S.R. Hurwitz, and J.R. Crandall, "Quantification of ankle articular cartilage topography and thickness using a high resolution stereophotography system," Osteoarthritis and Cartilage, vol. 15, pp. 205-211, 2007.
[16] K. Akiyama, T. Sakai, N. Sugimoto, H. Yoshikawa, and K. Sugamoto, "Three-dimensional distribution of articular cartilage thickness in the elderly talus and calcaneus analyzing the subchondral bone plate density," Osteoarthritis and Cartilage, vol. 20, pp. 296-304, 2012.
[17] Z. Li, J.E. Kim, J.S. Davidson, B.S. Etheridge, J.E. Alonso, and A.W. Eberhardt, "Biomechanical response of the pubic symphysis in lateral pelvic impacts: a finite element study," Journal of Biomechanics, vol. 40, pp. 2758-2766, 2007.
[18] M. N. Bajuri, M.R. Kadir, M.M. Raman, and T. Kamarul, "Mechanical and functional assessment of the wrist affected by rheumatoid arhtritis: A finite element analysis," Medical Engineering & Physics, vol. 34, pp. 1294-1302, 2012.
[19] F. Ezquerro, S. Jimenez, A. Perez, M. Prado, G. de Diego, and A. Simon, "The influence of wire positioning upon the initial stability of scaphoid fractures fixed using Kirschner wires: a finite element study," Medical Engineering & Physics, vol. 29, pp. 652-660, 2007.
[20] F.H. Netter, Atlas of human anatomy, Third ed. USA: ICON Learning System, 2003.
[21] H. J. Pfaeffle, M.M. Tomaino, R. Grewal, J. Xu, N.D. Boardman, S.L. Woo, and J.H. Herndon, "Tensile properties of the interosseous membrane of the human forearm," Journal Orthopaedic Research, vol. 14, pp. 842-845, 1996.
[22] S. Siegler, M.M. Tomaino, R. Grewal, J. Xu, N.D. Boardman, S.L. Woo, and J.H. Herndon, "The mechanical characteristics of the collateral ligaments of the human ankle joint," Foot & Ankle, vol. 8, pp. 234-242, 1988.
[23] A. Beumar, W.L. van Hemert, B.A. Swierstra, L.E. Jasper, and S.M. Belkoff, "A biomechanical evaluation of the tibiofibular and tibiotalar ligaments of the ankle," Foot & Ankle International, vol. 24, pp. 426-429, 2003.
[24] P. C. Liacouras and J. S. Wayne, "Computational modeling to predict mechanical function of joints: Application to the lower leg simulation of two cadaver studies," Journal of Biomechanical Engineering, vol. 129, pp. 811-817, 2007.
[25] M. K. Gislason, B. Stansfield, and D.H. Nash, "Finite element model creation and stability considerations of complex biological articulation: the human wrist joint," Medical Engineering & Physics, vol. 32, pp. 523-531, 2010.
[26] S. Nakamura, R.D. Crowninshield, and R.R. Cooper, "An analysis of soft tissue loading in the foot- a preliminary report," Bulletin of Prosthetics Research, vol. 18, pp. 27-34, 1981.
[27] H.-J. Kim, S.K. Kim, and S.H. Chang, "Bio-mechanical analysis of a fractures tibia with composite bone plates according to the diaphyseal oblique fracture angle," Composites Part B: Engineering, vol. 42, pp. 666-674, 2011.